Bioorganic & Medicinal Chemistry Letters 22 (2012) 4221–4224

Contents lists available at SciVerse ScienceDirect

Bioorganic & Medicinal Chemistry Letters

journal homepage: www.elsevier.com/locate/bmcl

Design, synthesis and biological evaluation of novel imidazopyridines as potential antidiabetic GSK3β inhibitors

Seung-Chul Lee [a,b], Hyun Tae Kim [a], Choul-Hong Park [a], Do Young Lee [a], Ho-Jin Chang [a], Soobong Park [a], Joong Myung Cho [a], Sunggu Ro [a,*], Young-Ger Suh [b,*]

[a] CrystalGenomics, Inc., 5F, Tower A, Korea Bio Park 694-1, Sampyeong-dong, Bundang-gu Seongnam-si Gyeonggi-do 463-400, Republic of Korea
[b] College of Pharmacy, Seoul National University, 599 Gwanak-ro, Gwanak-gu, Seoul 151-742, Republic of Korea

ARTICLE INFO

Article history:
Received 10 April 2012
Revised 14 May 2012
Accepted 15 May 2012
Available online 19 May 2012

Keywords:
Glycogen synthase kinase 3
Imidazopyridine
Type 2 diabetes mellitus
Oral glucose tolerance test

ABSTRACT

Design, synthesis and biological evaluation of the imidazopyridine analogs as novel GSK3β inhibitors for treatment of type 2 diabetes mellitus are described. Most of the analogs exhibited excellent inhibitory activities (IC50 < 44 nM) against glycogen synthase kinase 3β (GSK3β). The structure–activity relationship (SAR) of the imidazopyridine analogs and the binding mode of analog 23 in the catalytic domain of GSK3β, based on our X-ray crystallography study, are described. In particular, analog 28, which was selected as a potential drug candidate for treatment of type 2 diabetes mellitus, exhibited excellent GSK3β inhibition, pharmacokinetic profiles and blood glucose lowering effect in mouse.

Diabetes is a chronic disease characterized by peripheral insulin resistance and high concentrations of glucose in the blood. It generally results in decreased insulin secretion which could potentially cause serious debilitating conditions including cardiovascular morbidity, nerve damage, and mortality.[1] Although significant progress has been achieved in the treatment of type 2 diabetes mellitus (T2DM) over the last decade (Fig. 1), the biochemical and molecular mechanisms underlying insulin resistance have not been clearly defined yet.[2] In recent years, the biological and pharmacological researches revealed many targets for treatment of type 2 diabetes including glycogen synthase kinase 3 (GSK3). GSK3 is serine/threonine kinase originally identified as the enzyme responsible for inactivation of glycogen synthase.[3] It is involved in many different biological processes including glucose homeostasis, cell survival, tumorigenesis, Alzheimer's disease, and developmental patterning.[4]

We have recently reported the 7-hydroxy benzimidazole analogs, which exhibited excellent potency in both enzyme and cell based assay and high selectivity as GSK3β inhibitor.[5] However, the previous scaffold turned out unsatisfactorily for therapeutic implication in terms of physicochemical properties including polar surface area (PSA) value. Our strategy involved identifications of the potent and orally available GSK3β inhibitors via structural modification of the 7-hydroxy benzimidazole scaffold, which had been previously developed by us. In this context, we have initially attempted to modify the C7-hydroxy group, which seemed to function as both hydrogen-bonding donor and acceptor interacting with Asp133 and Val135 of the catalytic domain of GSK3β (Fig. 2).[5] It is well known that phenol bearing compounds undergo the phase 2 enzymatic metabolism. Therefore, we have decided to change the 7-hydroxy benzimidazole scaffold to the imidazopyri-

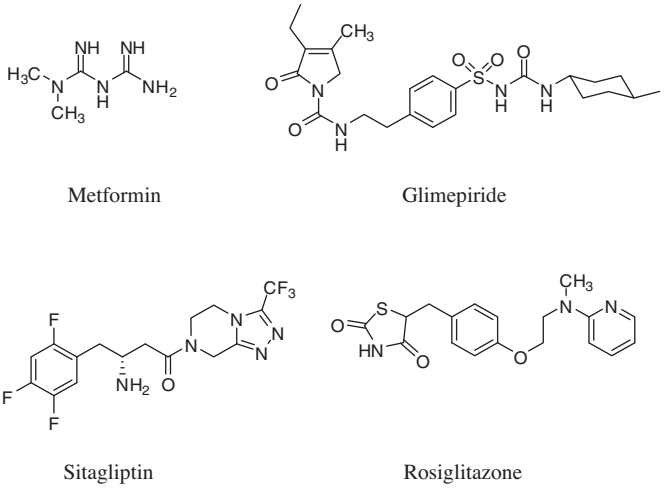

Figure 1. Examples of known hypoglycemic agents.

* Corresponding authors. Tel.: +88 31 628 2801; fax: +88 31 628 2701 (S.R.); tel.: +88 2 880 7875; fax: +82 2 888 0649 (Y.-G.S.).
E-mail addresses: sgro@cgxinc.com (S. Ro), ygsuh@snu.ac.kr (Y.-G. Suh).

0960-894X/$ - see front matter © 2012 Elsevier Ltd. All rights reserved.
http://dx.doi.org/10.1016/j.bmcl.2012.05.060

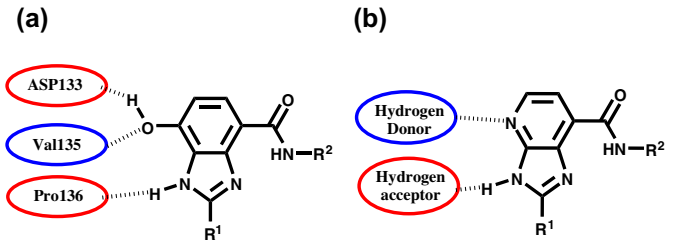

Figure 2. Proposed interaction of (a) the 7-hydroxy benzimidazole and (b) the imidazopyridine with GSK3β.

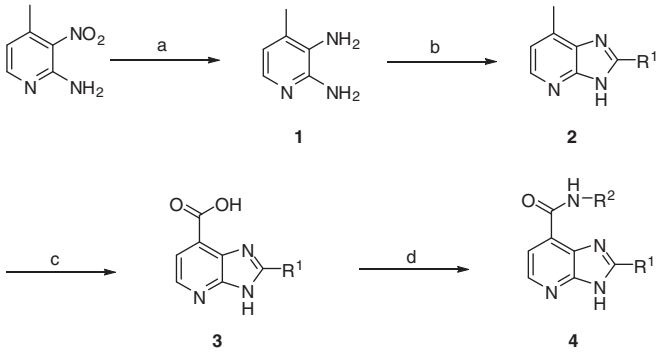

Scheme 1. Reagents and conditions: (a) Pd/C, H_2 balloon, MeOH, 5 h, 90–95%; (b) R^1-CHO, nitrobenzene, microwave irradiation, 50 W, 200 °C, 20 min; 70–95%; (c) $KMnO_4$, NaOH, H_2O, reflux, 12 h, 50–90%; (d) Pybop, Et_3N, R^2-NH_2, DMF, 2–10 h, 50–95%.

Table 1
Inhibitory activities of a 7-hydroxy benzimidazole analog and the imidazopyridine analogs against GSK3β

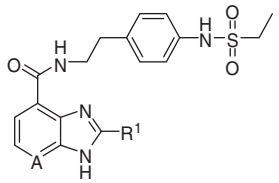

Analogs	A	R^1	IC_{50}, nM	EC_{50}, nM[a]
Ref. 14	—	—	70	ND
5	C–OH	Phenyl	47	ND
6	N	Phenyl	14	62
7	N	4-F-phenyl	4	31
8	N	2,4-di-F-phenyl	2	290
9	N	2-Thiophenyl	12	50
10	N	3-Thiophenyl	3	10
11	N	3-Furanyl	1	290

ND, not determined.
[a] EC_{50}s were determined by duplicate experiments using Rd cells and expressed as the mean.

dine scaffold, which has less molecular weight and is tolerable to potential glucuronidation.[6]

We have commenced the development of the novel GSK3β inhibitors by replacing the 7-hydroxy benzimidazole scaffold of the representative GSK3β inhibitor with the imidazopyridine scaffold. Representative synthetic route for variation of the R^1 and R^2-substituent is shown in Scheme 1. Analog 5 consisting of 7-hydroxy benzimidazole scaffold was synthesized to compare its GSK3β inhibitory activity with that of the corresponding analog consisting of the imidazopyridine scaffold. Commercially available 2-amino-3-nitro-4-methyl pyridine was converted into diamine 1 by palladium catalyzed reduction. Condensation of 1 with a variety of aldehyde under microwave irradiation at 200 °C afforded the corresponding imidazopyridine intermediate 2. Oxidation of **2** in the presence of $KMnO_4$ and NaOH in H_2O under the refluxing conditions afforded acid **3**. Amidation of **3** with an appropriate amine in the presence of Pybop and Et_3N in DMF yielded the corresponding imidazopyridine **4**. The GSK3β kinase inhibitory activity was determined using the known method[7] and the result is summarized in Table 1.

Interestingly, the imidazopyridine analog **6** (IC_{50} 14 nM) was more potent than the 7-hydroxy benzimidazole analog **5** (IC_{50} 47 nM). The other imidazopyridine analogs (**7**, **8**, **9**, **10** and **11**) exhibited excellent inhibitory activities in a range 1–12 nM.

The results implied that the imidazopyridine scaffold maintained a hydrophobic interaction even with the loss of a hydrogen-bonding interaction. In addition, our X-ray crystallographic data of the complex of GSK3β with analog **23** also revealed that the imidazopyridine interacted as a hydrogen-bonding donor and as a hydrogen-bonding acceptor, respectively with a carbonyl and an amino group of Val135.[8] The binding mode was quite similar to the results from recently reported our literatures.[5,9] The interaction of Asp133 with the hydroxy group shown in the benzimidazole scaffold disappeared as anticipated. Moreover, the interaction of C1-NH of the imidazole moiety with Pro136 changed to the interaction with Val135 (Fig. 3).

Based on the X-ray crystallographic analysis and the initial structure–activity relationship (SAR) of the imidazopyridine analogs, the R^1 and R^2-diversified analogs were synthesized and tested for the mouse and human microsomal stability. The selected analogs were incubated with human liver microsomes (HLMs) and mouse liver microsomes (MLMs) at 37 °C for 45 min. The inhibitory activities, the microsomal stability and the physicochemical properties of the imidazopyridine analogs are summarized in Table 2.

All analogs exhibited excellent inhibitory activities (IC_{50}s 9–44 nM) and acceptable cellular potencies (EC_{50}s 56–300 nM). From the mouse microsomal stability study, it was demonstrated that analogs **13** and **18** were metabolically stable (70% and 70.2%, respectively). However, analogs **16**, **17**, **19**, **20**, **21** and **18** showed polar characteristics with PSAs (125–156 Å^2), which seemed to unsatisfactory for oral absorption.[10]

Thus, we turned our attention to analog **13**, which not only had an acceptable cellular potency (EC_{50} 130 nM) and an excellent inhibitory activity (IC_{50} 8 nM) but also optimal physicochemical properties with a clogP (2.73) and a PSA (83.56 Å^2). Then, the analogs based on the structure of **13** were synthesized again. The sulfonamido and alkyl substituents were avoided in the second series of the imidazopyridine analogs because these increase PSA and molecular weight. The inhibitory activities, microsomal stabilities and physicochemical properties are summarized in Table 3.

The analogs bearing 3-diethylaminophenyl (**25**), 3-methoxy phenyl (**32**) and 3-pyridine (**31**) substituents exhibited excellent inhibitory activities (IC_{50}s 3 nM) as anticipated. However, they were unstable in the presence of both mouse microsome (0%, 6.4% and 6.3%) and human microsome (0%, 23.8% and 6.5%). In general, the imidazopyridine analogs showed low metabolic stability when the phenyl system with an electron-donating group at the meta-position or the 3-pyridinyl system was introduced as the R^1 moiety.

Although it exhibited lower potency than analog **27** in the cellular assay (EC_{50} 9 nM vs EC_{50} 1.5 nM), analog **26** consisting of the 4-methoxy-substituted pyridinyl system as R^2 moiety with metabolic stabilities of 87% (human) and 71% (mouse), was more stable than analog **27** consisting of the 4-ethoxy-substituted pyridinyl system with metabolic stabilities of 36% (human) and 38% (mouse). Analogs (**24**, **26**, **28**, **29**, **33** and **34**), which exhibited potent GSK3β inhibition, were subjected to pharmacokinetic study.

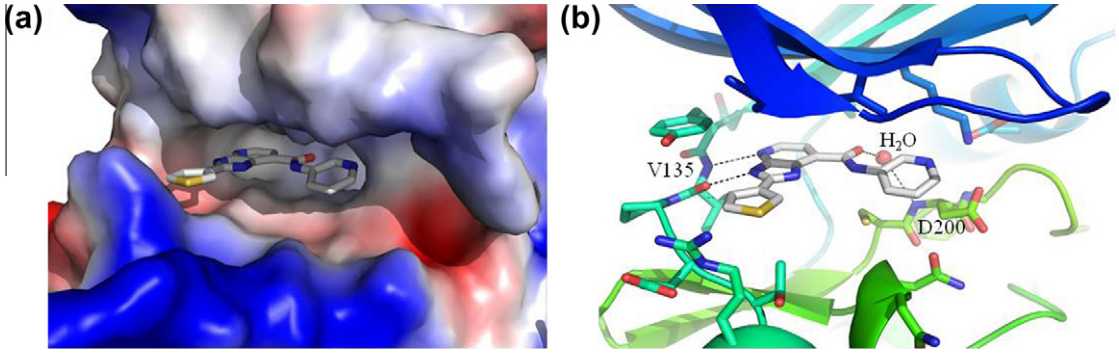

Figure 3. The X-ray crystallographic analysis of the interaction of analog **23** with the catalytic domain of GSK3β. The resolution is 2.6 Å, R value is 0.24 and R_free value is 0.304. The analog is illustrated in sticks with carbon atoms in white color. (a) Binding mode of the analog **23** in the ATP binding pocket of GSK3β was illustrated. (b) Hydrogen-bonding interaction is described. Interaction of amine of pyridine and NH of the imidazopyridine with NH of Val135, carbonyl of Val135 with distances of 3.0, 2.6 Å are shown. And carbonyl of amide linker interact with NH of Asp200 through water with distances of 2.5, 3.3 Å.

Table 2
Inhibitory activities against GSK3β, microsomal stabilities and physicochemical properties of the imidazopyridine analogs

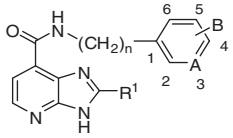

Analogs	R^1	R^2			IC_{50}, nM	EC_{50}, nM (Rd cells)	Metabolic stability[a] (microsome,%, 45 min)		*c*log*P*[b]	PSA[c], Å^2
		n	A	B			Mouse	Human		
12	4-F-phenyl	2	N	4-F	17	300	2.9	9.4	3.34	83.56
13	4-F-phenyl	0	N	—	8	130	70	ND	2.37	83.56
14	4-F-phenyl	3	N	4-Cl	17	250	4.2	25.7	3.63	83.56
15	4-F-phenyl	2	C	3-OH	14	150	11.1	12.1	3.28	90.90
16	4-F-phenyl	2	C	4-$NHSO_2CH_3$	44	190	0.8	13	1.95	125.22
17	4-F-phenyl	2	C	4-$NHSO_2N(CH_3)_2$	27	210	1.0	7.4	1.95	128.46
18	4-Cl-phenyl	2	C	4-$NHSO_2CH_3$	10	300	70.2	86.6	2.42	125.22
19	3-Furanyl	2	C	4-$NHSO_2CH_3$	3	180	5.2	47	0.95	138.36
20	2-Thiophenyl	2	C	4-$NHSO_2CH_3$	12	150	2.2	36.8	1.59	153.46
21	3-Thiophenyl	2	C	4-$NHSO_2N(CH_3)_2$	9	56	1.6	13.3	1.58	156.70
22	3-Furanyl	2	N	2-Cl	9	310	1.5	26.5	2.19	96.70

ND, not determined.
[a] Metabolic stability was determined by mass spectroscopy.
[b] clogP.
[c] PSA (polar surface area) was determined using MarvinSketch program.

Table 3
Inhibitory activities against GSK3β, microsomal stabilities and physicochemical properties of the imidazopyridine analogs based on **13**

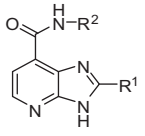

Analogs	R^1	R^2	IC_{50}, nM	EC_{50}, nM (Rd cells)	Metabolic stability (microsome, %, 45 min)		*c*log*P*[a]	PSA[b], Å^2
					Mouse	Human		
23	3-Thiophenyl	Pyridin-3-yl	13	240	ND	ND	2.01	111.80
24	4-Phenylpyrrolidine	4-Me-pyridin-3-yl	30	40	28.9	36.5	2.60	86.80
25	4-$(CH_3)_2$N-phenyl	4-Me-pyridin-3-yl	3	23	0	0	2.20	86.80
26	4-F-phenyl	4-OMe-pyridin-3-yl	3	9	87.0	71.0	2.21	92.79
27	4-F-phenyl	4-OEt-pyridin-3-yl	3	1.5	36.0	38.0	2.57	92.79
28	4-F-phenyl	6-Me-pyridin-3-yl	8	80	47.4	33.3	2.50	83.56
29	4-OMe-phenyl	4-Me-pyridin-3-yl	2	ND	56.8	51.4	1.93	92.79
30	3-OMe-phenyl	4-Me-pyridin-3-yl	3	ND	6.6	4.0	1.93	92.79
31	3-Pyridinyl	4-OEt-pyridin-3-yl	3	10	6.3	6.5	1.21	105.68
32	3-OMe-phenyl	4-OEt-pyridin-3-yl	7	10	6.4	23.8	2.27	102.02
33	3-Cl-phenyl	4-OMe-pyridin-3-yl	2	10	46.7	36.5	3.03	92.79
34	4-Pyridine	4-OMe-pyridin-3-yl	2	20	27.0	96.0	1.21	105.68

ND, not determined.
[a] clogP.
[b] PSA (polar surface area) was determined using MarvinSketch program.

Table 4
Pharmacokinetic profiles of the selected analogs[a]

Analogs	AUC[b] (ng/ml h)	C_{max} (ng/mL)	T_{max} (h)
24	39	–	–
26	545	228	1
28	2398	843	3
29	645	496	0.5
33	27	–	–
34	LLOQ[c]	–	–

Dose 27.3 mg kg^{-1}, ICR (Institute of cancer research) mice (n = 2, male), HCl salt formulation, Oral administration.
[a] Date were determined using WinNonline 5.3 program.
[b] AUC, area under curve.
[c] LLOQ, lower limit of quantitation.

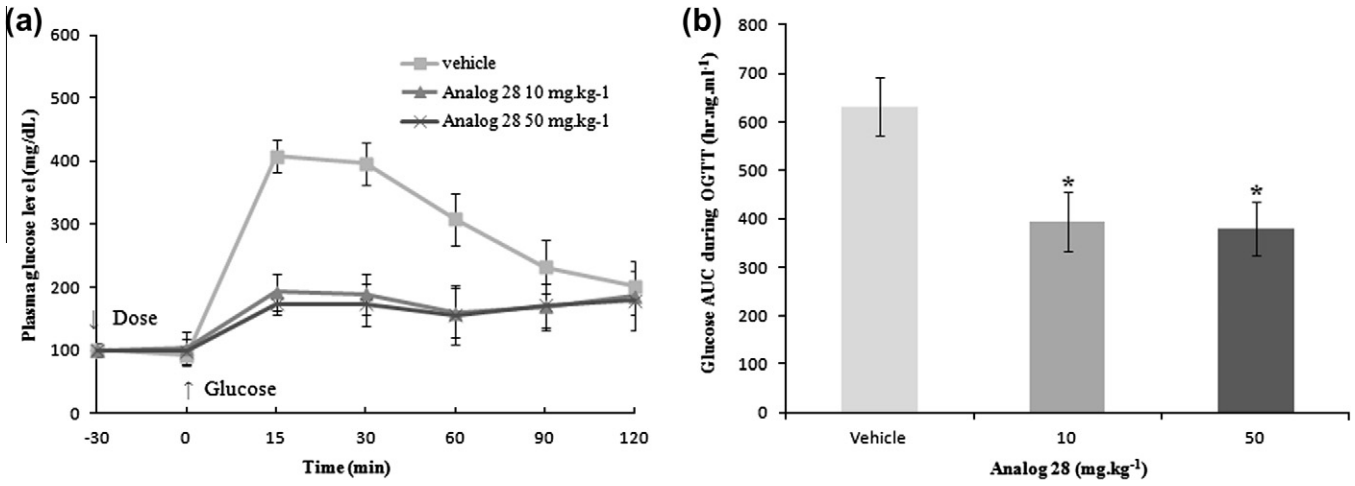

Figure 4. In vivo efficacy data of analog **28** in male mice OGTT (n = 5). The glucose was orally injected 30 min after oral administration of the suspension of analog **28** in PEG400. (a) Plasma glucose lowering effect and (b) glucose AUC reduction of analog **28**. *Values of $p < 0.05$ were considered statistically significant for vehicle group.

They were formulated as HCl salt for oral administration in ICR mice. The evaluation results are summarized in Table 4. Analog **28** showed the best oral exposure in the study. However, oral exposures of analogs **24**, **33** and **34** were unsatisfactory despite of their optimal physiochemical properties.

Based on many literature publications, GSK3 had been known as one of key mediators of insulin signaling pathway as it induces the glucose uptake, glycogen synthesis and lipid synthesis.[11] Therefore, we have further confirmed the pathophysiological relationship of the GSK3β inhibition through systemic glucose lowering effect of analog **28** in the oral glucose tolerance test (OGTT) using the ICR mice. The results are summarized in Figure 4. The glucose was orally injected after 30 min of administration of analog **28** and as expected, analog **28** effectively lowered the plasma glucose on the doses of 100 mg/kg and 10 mg/kg.[12]

These data suggested that GSK3β inhibitors could provide a potential therapeutic approach for treating type-2 diabetes.

In summary, we have designed and synthesized series of novel imidazopyridine analogs as excellent GSK3β inhibitors. We established the structure-activity relationship of the synthesized imidazopyridine analogs. The binding mode of the imidazopyridine analogs in the catalytic domain of GSK3β using analog **23** as a representative was elucidated via X-ray crystallography study. We were also able to identify potent GSK3β inhibitors that exhibited acceptable metabolic stabilities, physicochemical properties and promising pharmacokinetic profiles. In particular, analog **28** demonstrated effective blood glucose lowering effect in the OGTT using ICR mice. Currently, further biological and pharmacological studies on the selected analogs are in progress for the therapeutic implication.

References and notes

1. (a) Saltiel, A. R.; Kahn, C. R. *Nature* **2001**, *414*, 799; (b) Amos, A. F.; McCarty, D. J.; Zimmet, P. *Diabet. Med.* **1997**, *14*, 7; (c) King, H.; Aubert, R. E.; Herman, W. H. *Diabetes Care* **1998**, *21*, 1414.
2. (a) Williams-Herman, D.; Johnson, J.; Teng, R.; Luo, E.; Davies, M. J.; Kaufman, K. D. *Curr. Med. Res. Opin.* **2009**, *25*, 569; (b) Yoo, D. Y.; Kim, W.; Nam, S. M.; Yoo, M. H.; Hwang, I. K.; Yoon, Y. S. *Diabetes Care* **2010**, *36*, 2401; (c) Kus, V.; Flachs, P.; Kuda, O.; Bardova, K. *PLoS One* **2011**, *6*, e27126; (d) Sangle, G. V.; Lauffer, L. M.; Grieco, A. *Endocrinology* **2012**, *153*, 564.
3. Cohen, P.; Yellowlees, D.; Aitken, A.; Donella-Deana, A.; Hemmings, B. A.; Parker, P. j. *Eur. J. Biochem.* **1982**, *124*, 21.
4. Martinez, A.; Castro, A.; Dorronsoro, i.; Alonso, m. *Med. Res. Rev.* **2002**, *22*, 373.
5. Shin, D.; Lee, S. C.; Heo, Y. S.; Lee, W. Y. *Bioorg. Med. Chem. Lett.* **2007**, *17*, 5686.
6. Mutlib, A.; Goosen, T. C.; Bauman, J. N. *Chem. Res. Toxicol.* **2006**, *19*, 701.
7. (a) Gong, L.; Grupe, A.; Peltz, G. A. PCT Int. App. WO0210158, 2002.; (b) Cho, J. M.; Ro, S.; PCT Int. App. WO2004065370, 2004.
8. PDB ID code: 4DIT, title: Crystal structure of GSK3beta in complex with an imidazopyridine inhibitor.
9. Lee, S. C.; Shin, D.; Cho, J. M.; Ro, S.; Suh, Y. G. *Bioorg. Med. Chem. Lett.* **1891**, *2012*, 22.
10. (a) Ertl, P.; Rohde, B.; Selzer, P. *J. Med. Chem.* **2000**, *43*, 3714; (b) Lipinski, C. A.; Lombardo, F.; Dominy, B. W.; Feeney, P. J. *Adv. Drug Delivery Rev.* **2001**, *46*, 3.
11. Mohler, M. L.; He, Y.; Wu, Z.; Hwang, D. J.; Miller, D. D. *Med. Res. Rev.* **2009**, *29*, 125.
12. As demonstrated in many literatures, analog **28** also showed non-linear pharmacodynamics. It seems that the inconsistent solubility of analog **28** influenced the intestinal absorption, which resulted in an induction of non-linear pharmacodynamics. There is also a possibility of effects by the mouse efflux enzymes (e.g., Pgp). Currently, we try to solve the problem of non-linear pharmacodynamics via appropriate formulation. (a) Sparreboom, A.; Tellingen, O. V.; Nooijen, w. j. *Cancer Res.* **1996**, *56*, 2112; (b) Mueller, E. A.; Kovarik, J. M.; Bree, J. B.; Tetzloff, W.; Grevel, J. *Pharm Res.* **1994**, *2*, 301; (c) Kodell, R. L.; Turturro, A. *Nonlinearity Biol. Toxicol. Med.* **2004**, *2*, 35.